Hindawi
Mathematical Problems in Engineering
Volume 2018, Article ID 5148278, 12 pages
https://doi.org/10.1155/2018/5148278

Research Article

A Modified Walker Model Dealing with Mean Stress Effect in Fatigue Life Prediction for Aeroengine Disks

Shan Lu,[1] **Yunlai Su**,[1,2] **Mao Yang**,[1] **and Yan Li**[1]

[1] *School of Power and Energy, Northwestern Polytechnical University, Xi'an 710072, China*
[2] *AVIC Aircraft Strength Research Institute, Xi'an 710065, China*

Correspondence should be addressed to Shan Lu; shanlu@nwpu.edu.cn

Received 3 November 2017; Revised 27 January 2018; Accepted 31 January 2018; Published 22 March 2018

Academic Editor: Gregory Chagnon

Mean stress effect plays an important role in fatigue life prediction, and it is discovered that maximum stress has nonnegligible influence on mean stress effect. Therefore, a modified Walker model is proposed to account for mean stress effect on fatigue life of aeroengine disks, which contains the influence of stress ratio and maximum stress on mean stress effect. Eight sets of fatigue data for standard smooth bars from six kinds of materials commonly used in aeroengine disks as well as two sets of experimental data from simulated specimens of turbine disks were employed to investigate the prediction capability of the proposed model against other candidate mean stress relationships. It is found that Goodman model generates most conservative results, while Morrow model overestimates fatigue life for most cases. SWT model yields similar results to Walker model but with less accuracy. The results of the modified Walker model turn out to be superior to those of any other candidate models for all cases examined, especially for large mean stress ones. Thus, the modified Walker model can be an effective method to predict fatigue lives of aeroengine disks influenced by mean stresses.

1. Introduction

In aeroengine, most critical regions of disks are always subject to time varying loads with the presence of mean stresses. Many researchers have found that mean stresses have significant influence on fatigue life [1–5]. It is discovered that tensile mean stresses are usually detrimental to component fatigue while compressive mean stresses are beneficial in terms of fatigue strength. Besides, it is worth noting that mean stresses have significant effect on fatigue behavior in high cycle fatigue (HCF), while they have less influence in low cycle fatigue (LCF). This is because that large amount of plastic deformation will be generated in the LCF process, which will significantly reduce any beneficial or detrimental effect of the mean stresses [6].

In scientific researches, most fatigue tests are conducted particularly under completely reversed conditions with mean stresses being zero. Therefore, fatigue life predicting methods on the base of these fully reversed fatigue test data should be modified to account for mean stress effect for better accuracy. Since the fatigue process of a component consists of the crack initiation phase and the crack propagation phase, thus many researchers have proposed plenty of models to consider the mean stress effect on the crack initiation life and the crack propagation life separately. The commonly used FCG models considering mean stress effect on fatigue crack growth rate are Priddle model [7], Collipriest model [8], McEvily model [9], Forman model [10], and so on. These models are used in different situations and turn out to be effective [11]. As to the influence of mean stress on crack initiation life, there are many models proposed, like Goodman model [1], Gerber model, Morrow model [2], Manson-Halford model, the Smith-Watson-Topper (SWT) parameter [3], the Walker equation [5], the generalized energy damage parameter, and so on [12]. In this paper, we mainly focus on the effect of mean stress on crack initiation life, and the fatigue lives mentioned in rest of the paper are all crack initiation lives.

The prediction accuracy of the methods to assess mean stress effect on crack initiation behavior of various materials under different loading conditions has been investigated by Zhu et al. [12, 13], Correia et al. [14], Dowling et al. [15, 16], and Burger and Lee [17]. Zhu et al. [12, 13] have proposed the mean stress effect correction in fatigue life predictions based on energy parameters. Correia et al. [18, 19] proposed the generalization of the design fatigue life curve for several fatigue damage parameters including the Walker-like strain damage parameter and others with mean stress effects. Susmel [20] introduced a mean stress sensitivity index into the modified Wöhler curve method to account for the mean stress effect perpendicular to the critical planes under multiaxial loadings. Niesłony and Böhm [21] proposed a stress-based approach by employing two *S-N* curves under alternating stress and stress ratio $R = 0$. Kujawski [22] made use of analogy with Neuber's rule and proposed a deviatoric version of the SWT model to consider mean stress effect for relatively large compressive mean stress cases. Kamaya and Kawakubo [23] investigated the effects of mean stress on fatigue properties of type 316 stainless steel and indicated that mean stress correction was not necessary in component design under load control mode and for constrained ratcheting strain region. Ince [24] proposed a mean stress fatigue model based on the distortional strain energy to account for the mean stress effect on fatigue life for both positive and compressive mean stress conditions. Besides, researchers have proposed many other equations accounting for mean stress effects, some of which are discussed by Nihei et al. [25] and Kluger and Lagoda [26].

2. Mean Stress Models in Fatigue

Even though various models have been proposed to consider the mean stress effect, the Goodman model, Morrow model, SWT model, and Walker model are still considered to be most popular methods while predicting the crack initiation life in practical engineering. Therefore, these four mean stress models will be briefly illustrated as follows.

Goodman relationship employs the ultimate tensile strength, σ_u, as an important parameter together with mean stress σ_m and stress amplitude σ_a to obtain the equivalent stress σ_{ar}, as is shown in (1). However, the results from the Goodman method is found to be highly inaccurate [15, 27], especially for large mean stress cases.

$$\sigma_{ar} = \frac{\sigma_a}{1 - \sigma_m/\sigma_u}. \quad (1)$$

The Morrow equation shares the same form with Goodman's, except for employing the true fracture strength σ_f, instead of σ_u. In some cases, the true fracture strength may be unavailable. Therefore, an alternate form is proposed by substituting the fitting constant, σ_f', the stress intercept at $N_f = 0.5$ cycle of the *S-N* curve, to estimate the equivalent completely reversed stress amplitude at various stress ratios [28]. Both of the true fracture form and the stress intercept form of Morrow equation are shown in (2a) and (2b). The assumption of $\sigma_f' = \sigma_f$ is often accurate for steels, as shown by Landgraf [29]; however, for aluminums alloys the assumption shows less accuracy, as illustrated by Dowling et al. [15].

$$\sigma_{ar} = \frac{\sigma_a}{1 - \sigma_m/\sigma_f}, \quad (2a)$$

$$\sigma_{ar} = \frac{\sigma_a}{1 - \sigma_m/\sigma_f'}. \quad (2b)$$

The SWT method employs the maximum stress σ_{max} and the stress amplitude σ_a as parameters to calculate the equivalent completely reversed stress amplitude σ_{ar}, as is shown in (3). As can be seen, the SWT method has the advantage of simplicity and is not depending on any material constants. Besides, it is found that the SWT model provides good life prediction results in the long fatigue life region but is conservative in the low cycle fatigue life region [30, 31].

$$\sigma_{ar} = \sqrt{\sigma_{max}\sigma_a} = \sigma_a\sqrt{\frac{2}{1-R}} = \sigma_{max}\sqrt{\frac{1-R}{2}}. \quad (3)$$

Unlike the SWT method, the Walker model supposes that mean stress effect is material dependent. Thus, a fitting parameter γ, which varies from 0 to 1, is employed in the Walker equation to account for the variance of mean stress effect on different materials, as is shown in (4). The advantage of the Walker model is that it provides an opportunity to fit fatigue test data at various mean stresses all together, with γ being obtained as part of the fitting process. The higher γ is, the less sensitive of the material reacts to mean stress effect. On the contrary, a lower γ means that the material is more sensitive to mean stress effect [15].

$$\sigma_{ar} = \sigma_{max}^{1-\gamma}\sigma_a^{\gamma} = \sigma_a\left(\frac{2}{1-R}\right)^{1-\gamma} = \sigma_{max}\left(\frac{1-R}{2}\right)^{\gamma}. \quad (4)$$

It can be observed from the comparison between the SWT and the Walker model that when $\gamma = 0.5$, (4) is seen to reduce to (3), which means that the SWT equation is a special case of the Walker equation.

Basquin's equation [32] describes the relation of fatigue life and the equivalent fully reversed stress amplitude, which can be expressed as

$$\sigma_{ar} = \sigma_f'\left(2N_f\right)^b, \quad (5)$$

where σ_f' is the fatigue strength coefficient, b is the fatigue strength exponent, and N_f is the fatigue life. Usually, Basquin's equation is employed in conjunction with different mean stress models to estimate fatigue lives only with σ_{ar} being replaced.

3. The Proposed Model

From previous investigations, it is known that the Walker method gives better predictions than other models when fatigue data are available to fit the adjustable parameter γ [15–17, 33]. However, while employing the Walker model to estimate fatigue lives of some commonly used materials, such as FGH4095 powder metallurgy superalloy (600°C) and GH4169 wrought superalloy (650°C), it is noticed that the estimation results of the Walker equation distinctly changed from conservative to overestimated with the increase of stresses for large mean stress cases, which are shown in Figure 1. That is, for large mean stress cases, the Walker equation gives relatively conservative results in the low stress region; conversely, the estimated fatigue life results become nonconservative while the stresses are large, which certainly brings rather great errors.

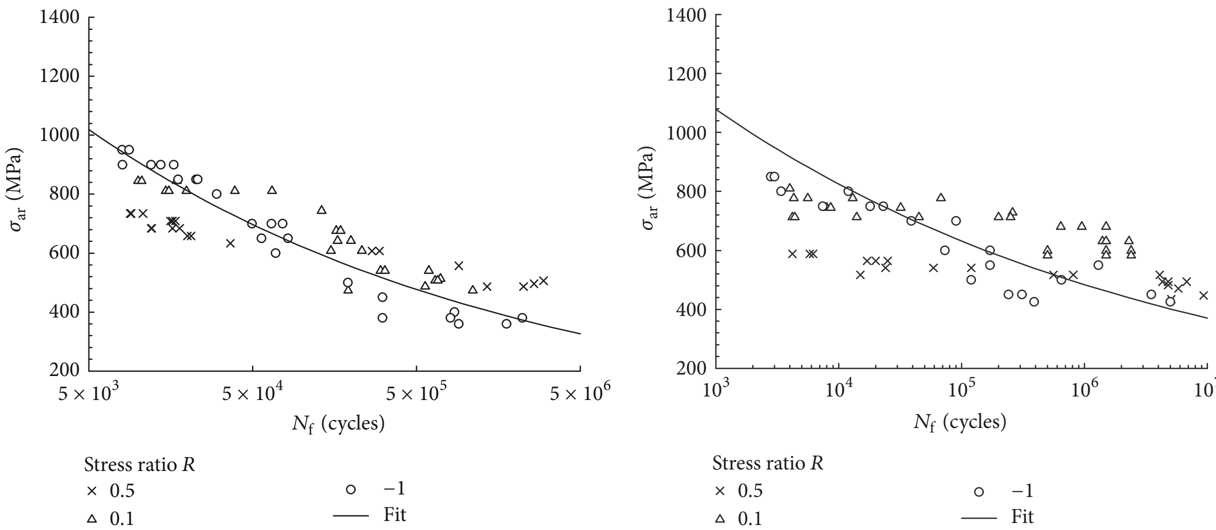

(a) Walker, FGH4095 600°C

(b) Walker, GH4169 650°C

Figure 1: Equivalent completely reversed stress amplitude versus fatigue life correlations by Walker model for the (a) FGH4095 superalloy (600°C) and (b) GH4169 superalloy (650°C).

Therefore, further researches were carried out to investigate the influence of maximum stress on mean stress effect. Based on the Walker model and Basquin's equation, the fitting parameter γ_i for each stress level $\sigma_{\max,i}$ is determined by the fatigue data on that stress level from different stress ratios through multiple linear regression, as is shown in (6), where α_1 and α_2 are the fitting results of Walker model for all data sets and will not change with different stress levels.

$$\log N_{f,i} = \alpha_1 + \alpha_2 \log \sigma_{\max,i} + \gamma_i \alpha_2 \log \frac{1-R}{2}. \qquad (6)$$

It can be obviously seen from Figure 2 that the fitting parameter γ varies with the change of logarithmic of maximum stress almost in a linear relationship for both FGH4095 and GH4169 superalloy. Since γ acts as an important index of mean stress effect in the Walker model, it can be deduced that maximum stress has nonnegligible influence on mean stress effect as well and should be involved while predicting fatigue life with mean stress effect for better accuracy. Thereupon the modified Walker model is proposed.

The equivalent completely reversed stress amplitude based on the proposed modified Walker model is shown in (7), in which the material dependent fitting parameter γ is replaced by $m+n\log\sigma_{\max}$ compared with Walker model, with one additional fitting parameter to account for the influence of maximum stress on mean stress effect. Therefore, the modified Walker model not only contains the influence of material on mean stress effect by employing parameter m, just as γ do in the Walker model, but also reflects the influence of maximum stress through parameter n. Taking the logarithm with base of 10 on the combination of (5) and (7), the modified Walker model can be expressed as (8), with β_i $(i = 1, 2, 3, 4)$ being the fitting results of multiple linear regression by all

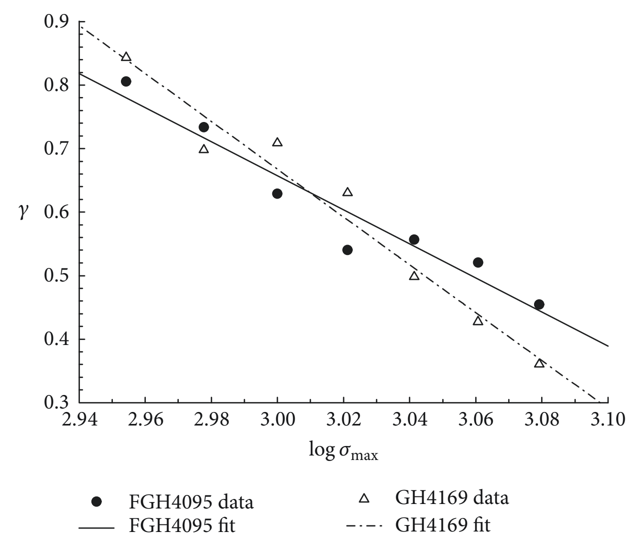

Figure 2: The influence of maximum stress on γ for FGH4095 (600°C) and GH4169 (650°C) superalloy.

data sets. Obviously, the parameters in (7) and (8) have the following relations: $m = \beta_3/\beta_2$, and $n = \beta_4/\beta_2$.

$$\sigma_{ar} = \sigma_{\max}\left(\frac{1-R}{2}\right)^{m+n\log\sigma_{\max}}, \qquad (7)$$

$$\log N_f = \beta_1 + \beta_2 \log\sigma_{\max} + \beta_3 \log\frac{1-R}{2} + \beta_4 \log\sigma_{\max} \log\frac{1-R}{2}. \qquad (8)$$

Though the modified Walker equation contains two fitting parameters while the Walker equation merely includes

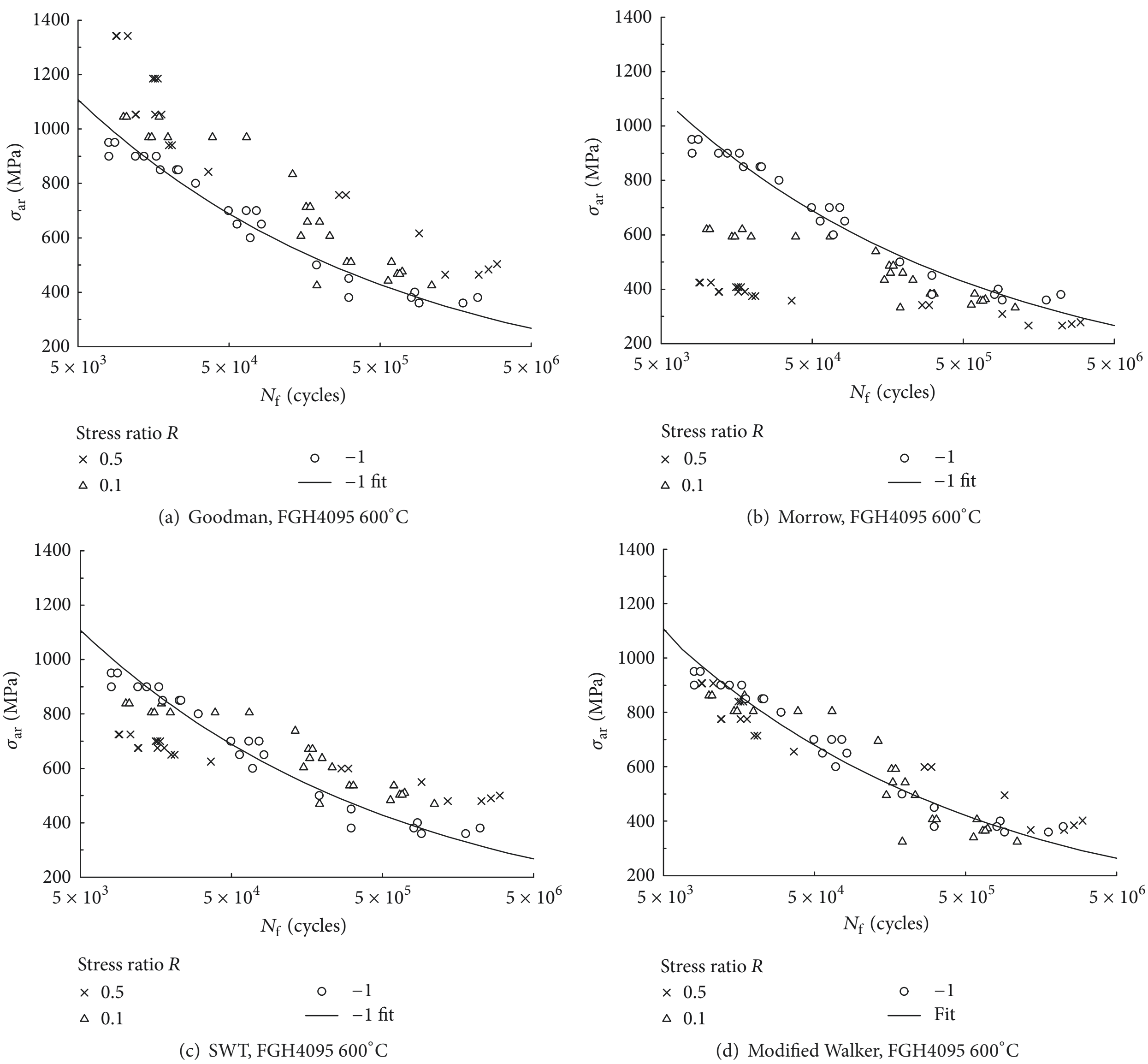

(a) Goodman, FGH4095 600°C

(b) Morrow, FGH4095 600°C

(c) SWT, FGH4095 600°C

(d) Modified Walker, FGH4095 600°C

Figure 3: Equivalent completely reversed stress amplitude versus fatigue life correlations for FGH4095 superalloy (600°C) for the (a) Goodman, (b) Morrow, (c) SWT, and (d) modified Walker methods.

one, the determination of the two parameters in modified Walker equation is not complicated compared to that of the one parameter in Walker equation. Since (7) shares the same form as (4), there is no difference in the multiple linear regressions of fatigue test data at various mean stresses for the Walker model and modified Walker model. The fitting process of the Walker model has been specifically demonstrated by Dowling et al. in [15]; therefore it will not be repeated here.

4. Validation

4.1. Comparison of Mean Stress Models with Experimental Data from Standard Smooth Bars. Fatigue test data of standard smooth bars for various stress ratios are employed to verify the prediction capability of the candidate mean stress models in (1) to (4) and (7) by plotting the equivalent fully reversed stress amplitude σ_{ar} versus fatigue life N_{f}. In what follows, σ_{ar} of each test data point is calculated by the corresponding mean stress equations mentioned previously.

The plots of σ_{ar} versus N_{f} for FGH4095 (600°C) and GH4169 (650°C) superalloy are shown in Figures 3 and 4 separately, which include the results of Goodman model, Morrow model, SWT model, and the modified Walker model, respectively (the results of Walker model have been plotted in Figure 1 already). In each plot, the degree of resulting data points which consolidate with the fitted line gives an indication of the success of the mean stress relationship. It should be noted that the fitted lines in the Goodman model, Morrow model, and SWT model are obtained just from the fatigue test data of $R = -1$ (or $\sigma_{\mathrm{m}} = 0$), while the fitted lines

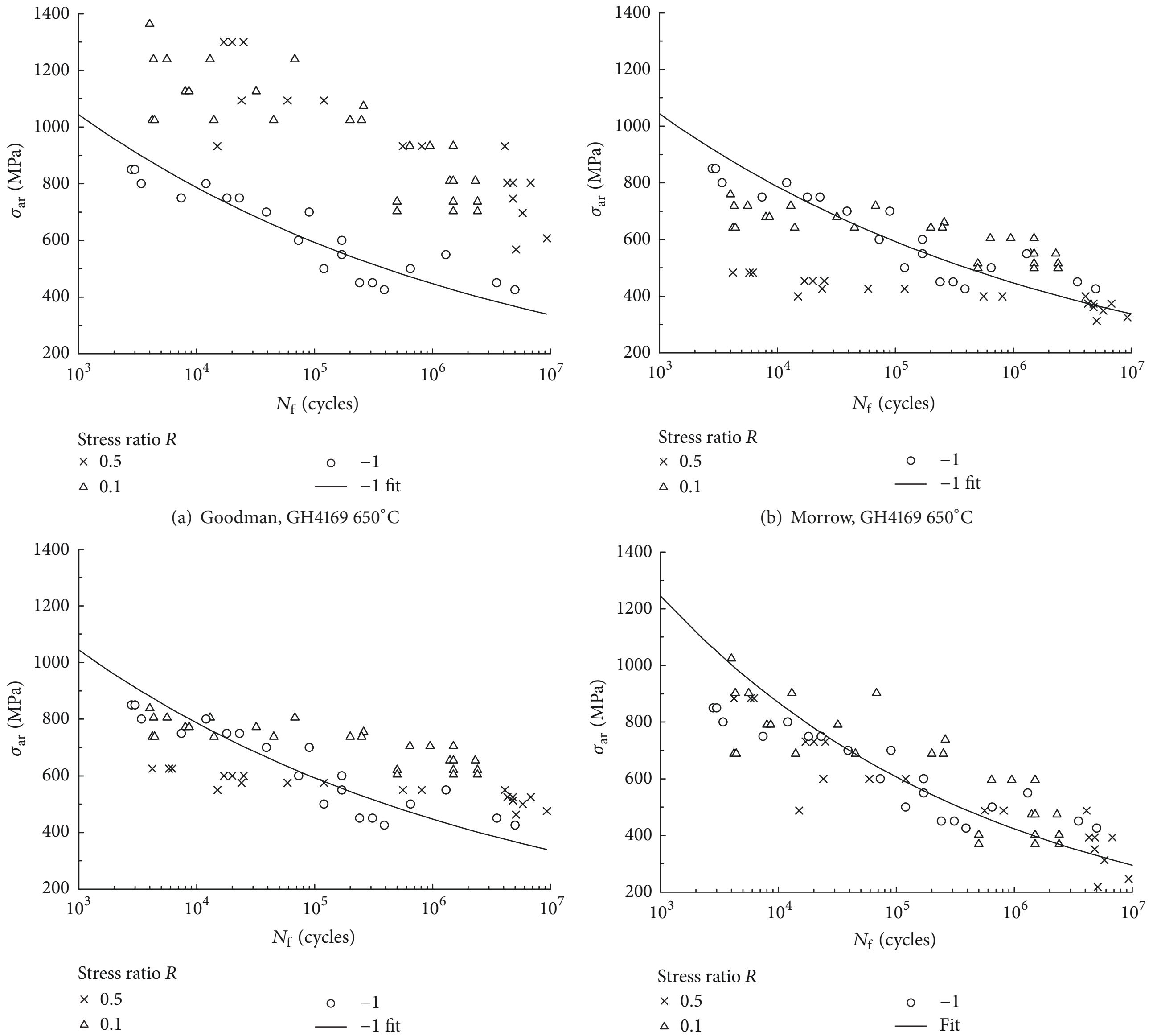

(a) Goodman, GH4169 650°C

(b) Morrow, GH4169 650°C

(c) SWT, GH4169 650°C

(d) Modified Walker, GH4169 650°C

Figure 4: Equivalent completely reversed stress amplitude versus fatigue life correlations for GH4169 superalloy (650°C) for the (a) Goodman, (b) Morrow, (c) SWT, and (d) modified Walker methods.

of the Walker model and modified Walker model result from fitting the data sets at all mean stresses.

For FGH4095 superalloy (600°C), it can be recognized in Figure 3(a) that the data of stress ratio $R = 0.5$ distribute far above the fitted line of data $R = -1$ in the Goodman relation plot, and the data set of stress ratio $R = 0.1$ also distribute above the fitted line, but they lie comparatively closer than the $R = 0.5$ data set, which indicates that the Goodman relationship is applicable to estimate fatigue life for small mean stress cases; however when the mean stress gets larger, Goodman relation becomes highly inaccurate, and the larger the mean stress is, the less the accuracy may become. The results of Morrow equation for $R = 0.5$ and $R = 0.1$ data sets distribute below the zero mean stress line. Similarly, the results of $R = 0.1$ data set lie much closer than that of $R = 0.5$ data set. In Figure 3(c), reasonable results are obtained by the SWT model, which show better accuracy than the Goodman and Morrow relations. Furthermore, it is discovered that the Walker model provides slightly better results than the SWT model through comparison of Figures 1(a) and 3(c), which can be attributed to the adjustable fitting parameter γ by varying the resulting curve to fit data in cases where the SWT method is not very accurate [15]. Meanwhile, it is observed that either SWT or Walker model provides conservative results in the low stress region for large mean stress cases, while in the high stress region the opposite happens. Compared with other plots in Figures 1 and 3, it can be clearly observed that the modified Walker model

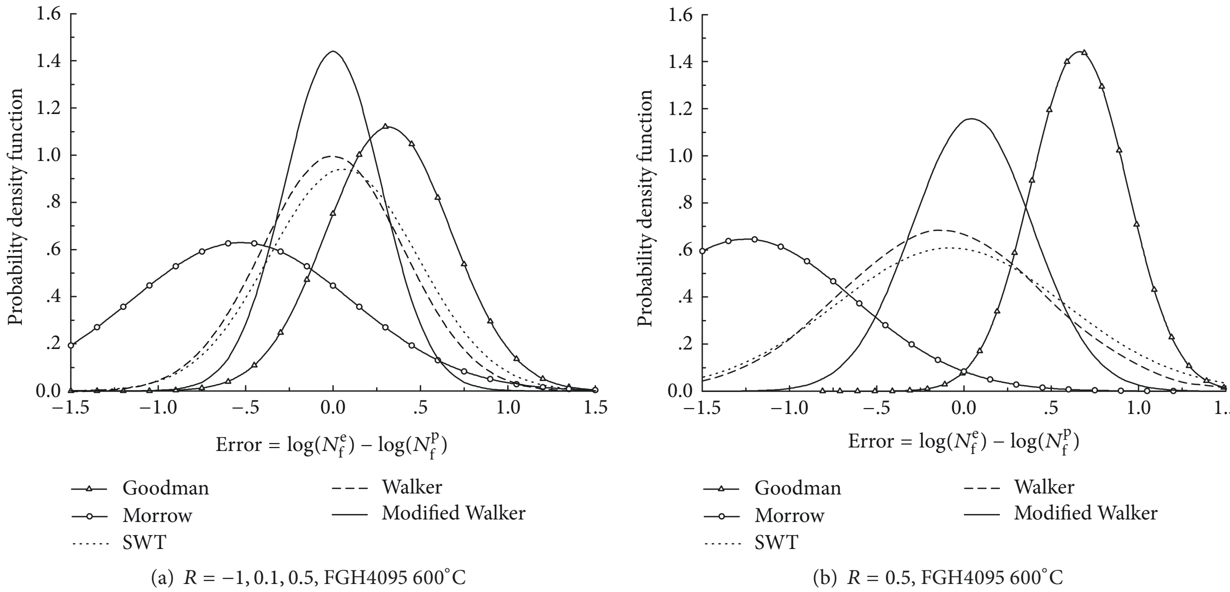

Figure 5: Probability density function of prediction errors of FGH4095 superalloy (600°C) for the data set of (a) all data set and (b) $R = 0.5$ data set.

with the consideration of mean stress effect on fatigue life influenced by both materials and maximum stresses gives superior results, which is illustrated by the fatigue test data of all stress ratios in Figure 3(d) which basically equally distribute on both sides of the fitted line.

Similar conclusions can be drawn for GH4169 superalloy (650°C) in Figure 4; only the results of Goodman model distributed much far from the fitted line than Morrow model for data sets of $R = 0.5$ and $R = 0.1$.

To quantitatively summarize the accuracy of the mean stress equations for different materials, the difference between the experimental logarithmic life and predicted logarithmic life for fatigue data sets is taken to calculate the prediction error of each model, which can be expressed as

$$\text{error} = \log\left(N_f^e\right) - \log\left(N_f^p\right), \quad (9)$$

where N_f^e is the experimental fatigue life and N_f^p is the predicted fatigue life of a given data point. Obviously, a positive error means that the prediction is conservative, while a negative error indicates the prediction is overestimated.

Besides, a probabilistic method is applied to analyze the prediction errors in the form of fitted probability density functions (PDF). The mean and standard deviation values are effective parameters to illustrate the prediction accuracy of different models. The fitted PDFs for prediction errors of each mean stress relationship are shown in Figures 5 and 6 for FGH4095 (600°C) and GH4169 (650°C) superalloy, separately. As clearly seen in Figure 5, the Goodman model tends to provide conservative predictions with positive mean values of prediction error for FGH4095 superalloy (600°C). On the contrary, the Morrow model tends to overestimate fatigue lives with negative errors. Besides, the standard deviations of Morrow model are comparatively large, which indicates that the prediction accuracy of Morrow model shows less stability. The results of SWT model and Walker model share the same tendency, while the Walker model provides slightly better results with larger probability to locate near the zero-error region. It can be seen that the modified Walker model shows best performance with mean values around zero and small standard deviations compared with other mean stress models. Particularly for the large mean stress cases like $R = 0.5$ data set, the modified Walker model provides much better results than other models.

The prediction accuracy of each mean stress model for GH4169 superalloy is similar to that of FGH4095 superalloy. Only the Goodman model shows less accuracy while Morrow model brings better results compared with FGH95 superalloy. Similarly, the modified Walker model provides better results than SWT and Walker models, even though these two models show much better results than the Goodman and Morrow models.

Besides the FGH4095 (600°C) and GH4169 (650°C) superalloy, some other materials which are commonly used in aeroengines such as FGH4095 (500°C), GH4169 (500°C), and FGH4096 superalloy [34], TC11 titanium alloy and 35Cr2Ni4MoA high-strength steel [35], and 2014-T6 aluminum [36] are also employed to demonstrate the accuracy of the mean stress models. The material properties and the fitting constants of Basquin's, Walker, and modified Walker equations are shown in Table 1. It should be noted that the parameters in Table 1 are determined by the analysis of fatigue data in corresponding references.

The plots of σ_{ar} versus N_f by the newly proposed modified Walker model for other materials examined in this study are shown in Figure 7. Besides, the mean and standard deviation values of prediction errors for all the materials examined are shown in Table 2, in which μ stands for mean value while σ is standard deviation value of the prediction errors. It should be

Table 1: Material properties and parameters for mean stress models.

Material	Source[a]	Temperature °C	Ultimate σ_u, MPa	Basquin σ_f', MPa	Basquin b	Walker γ	Modified Walker m	Modified Walker n
FGH4095	[34]	500	1490	7634	−0.2077	0.5784	4.9349	−1.4204
		600	1480	7422	−0.2065	0.4907	6.5782	−1.9737
GH4169	[34]	500	1230	5187	−0.1729	0.6772	9.5177	−2.8557
		650	1170	2654	−0.1228	0.5442	19.0449	−6.0689
FGH4096	[34]	550	1450	4519	−0.1546	0.6465	2.6067	−0.6894
TC11	[35]	300	830	1734	−0.1051	0.4403	5.5861	−1.7912
35Cr2Ni4MoA	[35]	160	1070	1342	−0.0584	0.3784	9.7109	−3.0370
2014-T6 Al	[36]	/	494	1120	−0.1221	0.4815	2.3949	−0.7241

[a]Numbers refer to the list of references at the end of the paper.

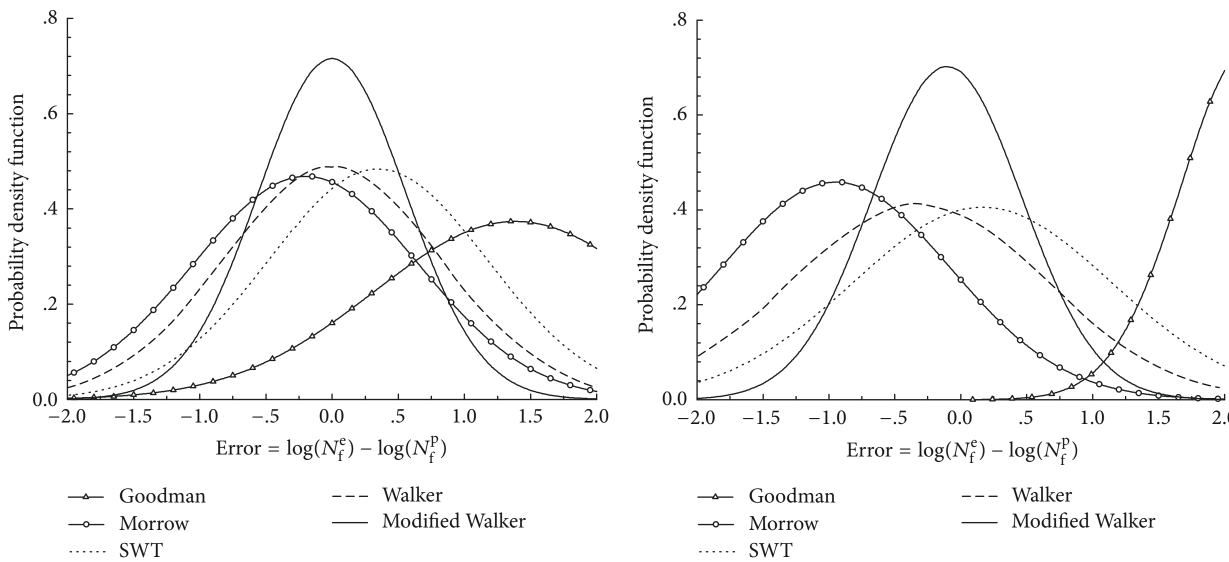

(a) $R = -1, 0.1, 0.5$, GH4169 650°C

(b) $R = 0.5$, GH4169 650°C

Figure 6: Probability density function of prediction errors of GH4169 superalloy (650°C) for the data set of (a) all data set and (b) $R = 0.5$ data set.

noted that all the μ and σ in Table 2 are obtained by all stress ratio data sets.

By analyzing plots in Figure 7 as well as the mean and standard deviation values in Table 2 for all the materials examined, it can be seen that the results of candidate mean stress models for the materials examined share the same tendency with FGH4095 and GH4169 superalloy. That is, the Goodman relation gives the most conservative results with positive mean values of error, while Morrow model overestimates the fatigue life for most cases. Besides, the standard deviation values of both Goodman and Morrow are comparatively large, which indicates that the prediction accuracy of these two models varies strongly. SWT model, as a special case of Walker equation, fails to reflect the influence of different materials on mean stress effect and thus provides less prediction accuracy than the Walker equation. The modified Walker model brings the least standard deviation values as well as mean values of error being zero, showing favorable capability to estimate fatigue lives for different materials and different mean stress cases. As to the zero values for μ in the Walker and modified Walker models, because both the Walker and modified Walker model determine parameters through multiple linear regression of all stress ratio data sets, which is essentially based on the least squares principle, there is no wander that the mean values of prediction errors for the Walker and modified Walker model become zero.

4.2. Comparison of Mean Stress Models with Experimental Data from Simulated Specimens. The previous work has proved that the modified Walker model provides favorable results for standard smooth bars of all materials examined. However, it remains to be testified whether the modified Walker model is applicable to estimate fatigue lives of real components in aeroengine. Therefore, two sets of experimental data from a type of simulated bolt-hole specimen and a type of simulated run-way hole specimen of turbine disk at

Table 2: Statistical analysis for the prediction errors of different mean stress methods for all materials examined.

Material	$T/^{\circ}C$	Goodman		Morrow		SWT		Walker		Modified Walker	
		μ	σ	μ	σ	μ	σ	μ	σ	μ	σ
FGH4095	500	0.3230	0.3817	−0.4136	0.5109	0.1462	0.4195	0	0.3491	0	0.2552
	600	0.3185	0.3557	−0.5253	0.6334	0.0603	0.4235	0	0.4008	0	0.2769
GH4169	500	1.0847	1.2153	−0.1752	0.7362	0.3505	0.7548	0	0.7093	0	0.6264
	650	1.3863	1.0668	−0.1981	0.8512	0.3472	0.8241	0	0.8177	0	0.5570
FGH4096	550	0.1990	0.2909	−0.2030	0.3114	0.1567	0.2915	0	0.2496	0	0.2275
TC11	300	0.6449	0.7774	−0.5057	0.7527	−0.0278	0.5372	0	0.5207	0	0.4510
35Cr2Ni4MoA	160	2.6252	2.7821	0.9583	0.9327	−0.0390	0.7505	0	0.6306	0	0.3567
2014-T6 Al	/	0.4311	0.5573	−0.5291	0.4601	0.0233	0.2884	0	0.2575	0	0.2212

Table 3: Main geometric parameters for the two simulated specimens of turbine disk.

Parameters	$R1$	$L1$	$R2$	$W1$	W	L	$H1$	$H2$
Bolt-hole specimen/mm	3.0	/	8.25	12.0	34.5	113.0	4.0	6.0
Run-way hole specimen/mm	3.2	4.2	8.25	11.2	34.2	126.4	4.0	6.0

Table 4: The comparison of estimated results of each mean stress models versus experimental data for simulated specimens.

Specimen	Experimental fatigue lives	Median fatigue life	Predicted fatigue lives				
			Goodman	Morrow	SWT	Walker	M. Walker
Bolt-hole specimen	20546, 24287, 15746, 8689, 24644, 9601, 25162	16977	28047	35276	13234	20276	14976
Error		/	65.2%	107.8%	−22.0%	19.4%	−11.8%
Run-way hole specimen	14572, 26378, 60050, 53267, 151668, 51627, 46216, 28838, 8079, 12174, 13368	29867	10823	48642	19569	21015	21188
Error		/	−63.8%	62.9%	−34.5%	−29.6%	−29.1%

550°C are analyzed to investigate the prediction capability of candidate models. The main geometric parameters of the two specimens are shown in Table 3 and the finite element (FE) models of the two specimens are shown in Figure 8.

The finite element analysis (FEA) results of the two specimens are shown in Figure 9. It should be noted that Figure 9 shows the contour plot of modified Walker equivalent stress for the two simulated specimens. Since both of the critical regions in the two specimens are obviously notched, the theory of critical distances (TCD) should be employed to properly accounting for the detrimental effect of stress concentration, and the line method (LM) of TCD is found to be an effective method [37]:

$$\sigma_{\text{eff}} = \frac{1}{L_{\text{eff}}} \int_0^{L_{\text{eff}}} \sigma(r, \theta = 0)\, dr, \tag{10}$$

where r and θ are the polar coordinates of the stress point from the critical point, with the stress gradient being the r axis, and L_{eff} is the distance from the notch tip to the minimum of relative stress gradient χ, as is shown in

$$\chi = \frac{1}{\sigma(r, \theta = 0)} \cdot \frac{d\sigma(r, \theta = 0)}{dr}. \tag{11}$$

The predicted fatigue life of the two simulated specimens can be obtained by modified Walker model in conjunction with LM, as is shown in Table 4. Besides, the predicted lives by other models and experimental fatigue lives of the two specimens are also provided for comparison. Obviously, the modified Walker model provides superior results than any other models for both of the two types of simulated specimens. Although the Walker model also gives reasonable fatigue life estimation, it still shows less accuracy for failing to reflect the effect of maximum stress on mean stress effect. Morrow model overestimates the fatigue lives while SWT model generates conservative results for both of the two specimens.

5. Conclusions

To comprehensively account for the influence of stress ratio, material, and maximum stress on mean stress effect, the modified Walker model is proposed. Then, eight sets of experimental data from standard smooth bars of six different materials and two sets of fatigue test data from simulated bolt-hole and runway-hole specimens of a turbine disk have been employed to investigate the prediction capability of the proposed model against other mean stress relationships commonly used. The results of the modified Walker model turn out to be superior to other candidate models for all materials examined. Goodman model is found to be

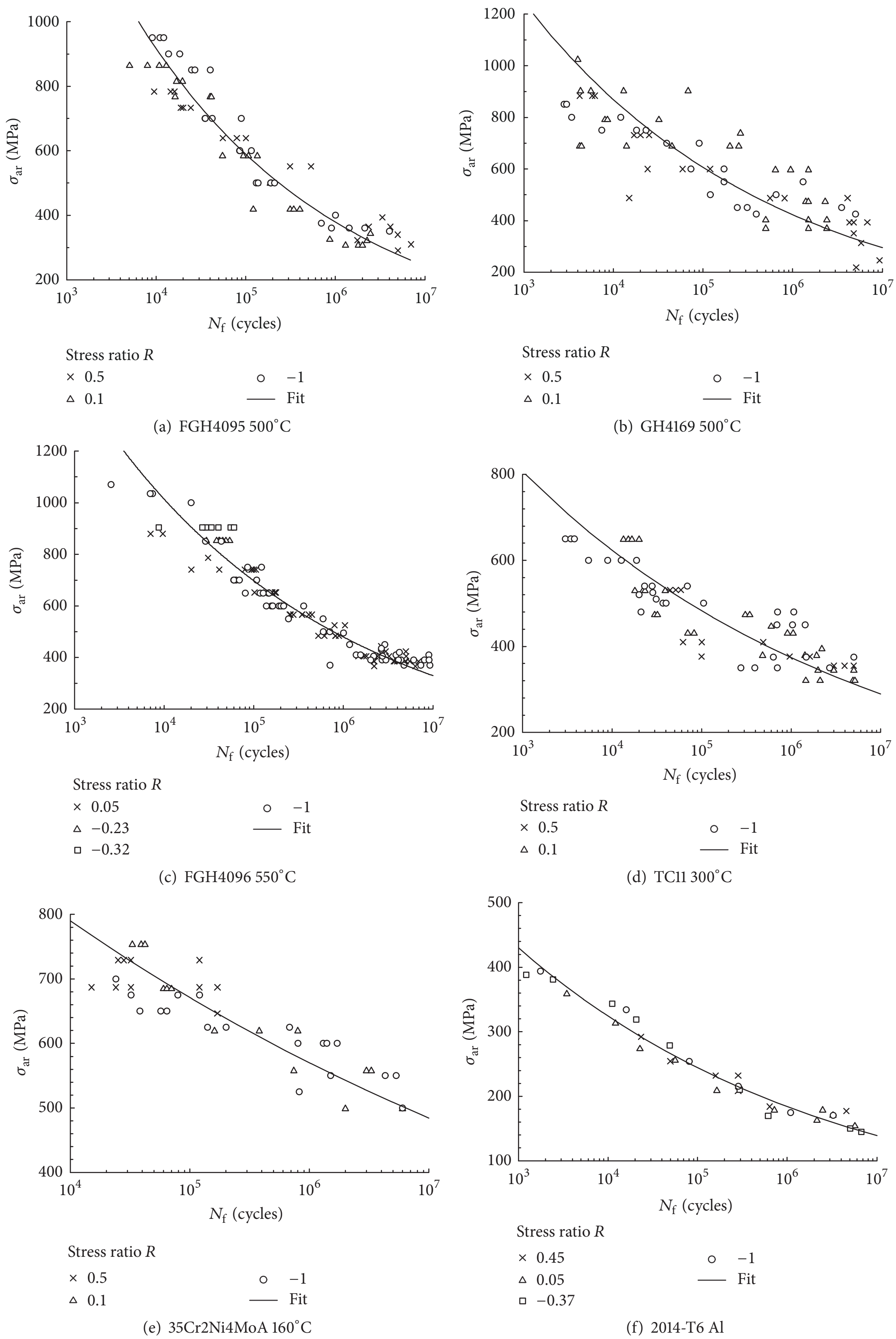

FIGURE 7: Equivalent completely reversed stress amplitude calculated by modified Walker model versus fatigue life for (a) FGH4095 superalloy (500°C), (b) GH4169 superalloy (500°C), (c) FGH4096 (550°C) superalloy, (d) TC11 alloy (300°C), (e) 35Cr4Ni2MoA steel (160°C), and (f) 2014-T6 aluminum.

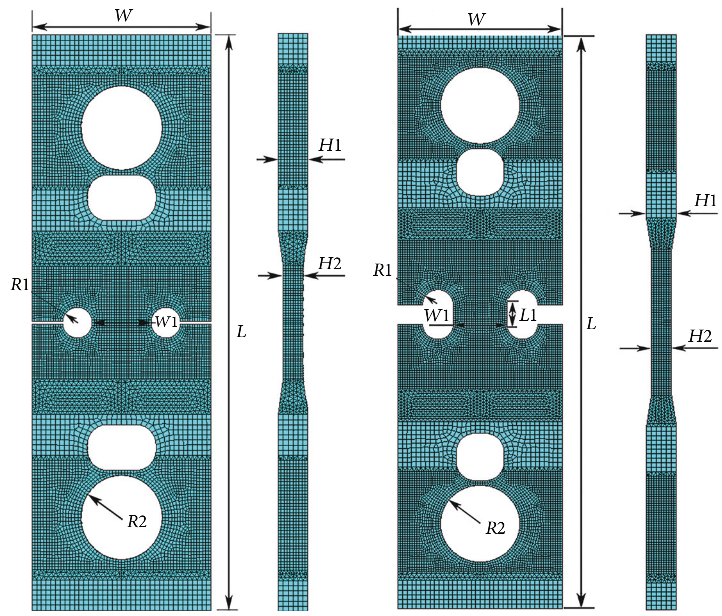

(a) Bolt-hole specimen (b) Run-way hole specimen

FIGURE 8: The finite element model for (a) bolt-hole simulated specimen and (b) run-way hole simulated specimen.

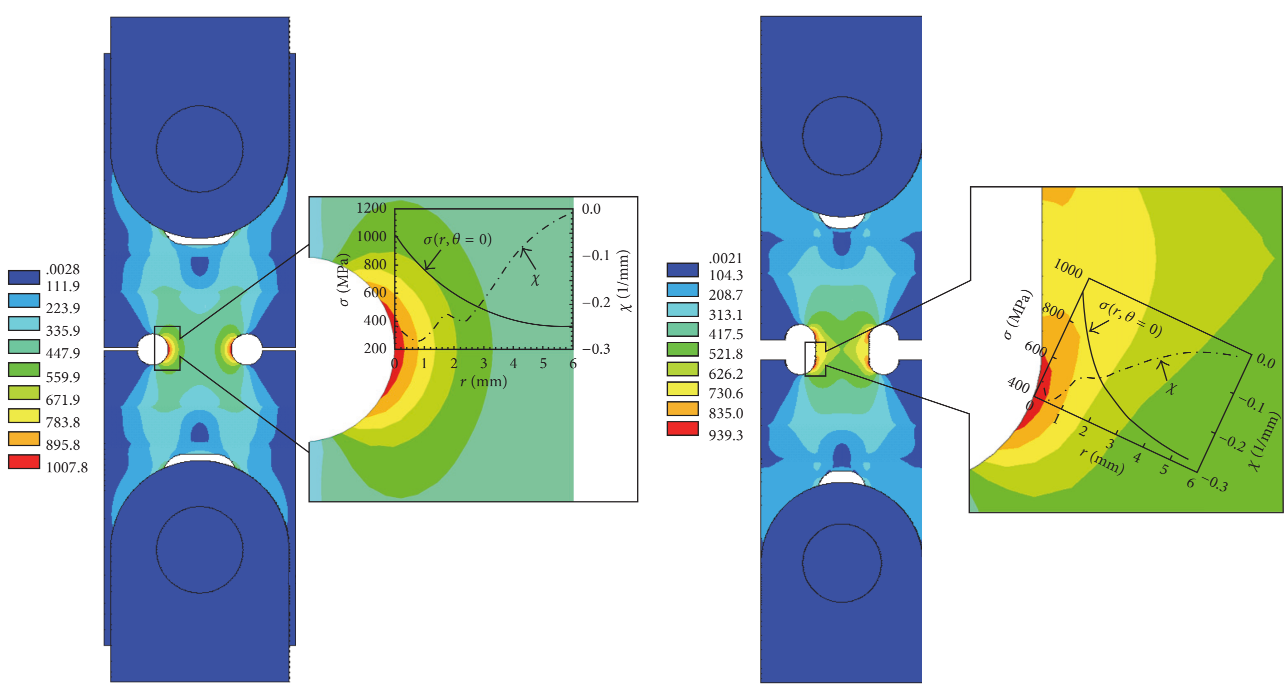

(a) (b)

FIGURE 9: The contour plots of modified Walker equivalent stress and relative stress gradients along the stress gradient path of the critical regions for (a) bolt-hole specimen and (b) runway-hole specimen.

most inaccurate, and Morrow equation shows better results than Goodman model. However, the results of the two models are both far from satisfactory. The SWT model brings reasonable results; what is more, it has the advantage of brevity; therefore, the SWT method is a good choice for general use. The Walker model provides satisfactory performance when mean stresses are relatively small by employing a material dependent parameter γ; however, it fails to correlate the fatigue data well for the large mean stress cases.

The proposed modified Walker model is based on the Walker model with an extra item of stress and stress ratio. Thus the modified Walker model inherits the advantage of Walker model and contains the influence of maximum stress on mean stress effect as well, showing favorable capability to estimate fatigue lives for different materials and different mean stress cases, sharing the same data pool and procedure to determine the fitting parameters, without increasing the calculation cost. Even though being a little complicated than the Walker model, the modified Walker model gives more precise results than the Walker model for all data sets examined, especially in large mean stress cases, showing better accuracy and larger scope of application.

Conflicts of Interest

The authors declare that there are no conflicts of interest regarding the publication of this paper.

Acknowledgments

The authors gratefully acknowledge the support from the China Gas Turbine Establishment.

References

[1] J. Goodman, *Mechanics Applied to Engineering. Longmans*, Longmans, Green and Co., London, UK, 1919.

[2] J. Morrow, “Fatigue properties of metals, section 3.2,” in *Fatigue Design Handbook, Pub. No. AE-4*, Society of Automotive Engineers, Warrendale, Pa, USA, 1968, Section 3.2 is a summary of a paper presented at Division 4 of the SAE Iron and Steel Technical Committee, Nov. 4, 1968.

[3] K. N. Smith, P. Watson, and T. H. Topper, “Stress- strain function for the fatigue of metals,” *Journal of Materials*, vol. 5, no. 4, pp. 767–778, 1970.

[4] K. Walker, “The effect of stress ratio during crack propagation and fatigue for 2024-T3 and 7075-T6 aluminum,” in *Effects of Environment and Complex Load History on Fatigue Life*, ASTM STP 462. American Society for Testing and Materials, pp. 1–14, Philadelphia, Pa, USA, 1970.

[5] N. E. Dowling, “Mean stress effects in stress-life and strain life fatigue,” in *Proceedings of Fatigue 2004: Second SAE Brazil International Conference on Fatigue*, Sao Paulo, Brazil, June 2004, Also SAE Paper No. 2004-01-2227, SAE International, Warrendale, PA, 2004.

[6] Y. L. Lee, M. E. Barkey, and H. T. Kang, “Metal fatigue analysis handbook: practical problem-solving techniques for computer-aided engineering,” pp. 151–157, Butterworth-Heinemann Press, UK, 2011.

[7] E. K. Priddle, “High cycle fatigue crack propagation under random and constant amplitude loadings,” *International Journal of Pressure Vessels and Piping*, vol. 4, no. 2, pp. 89–117, 1976.

[8] J. E. Collipriest, R. M. Ehret, and C. Thatcher, “Fracture mechanics equations for cyclic growth,” Tech. Rep. MFS-24447, NASA Technology Utilization Report, 1973.

[9] A. J. McEvily, D. Eifler, and E. Macherauch, “An analysis of the growth of short fatigue cracks,” *Engineering Fracture Mechanics*, vol. 40, no. 3, pp. 571–584, 1991.

[10] R. G. Forman, V. E. Kearney, and R. M. Engle, “Numerical analysis of crack propagation in cyclic-loaded structures,” *Journal of Basic Engineering*, vol. 89, no. 3, pp. 459–463, 1967.

[11] K. S. Al-Rubaie, E. K. L. Barroso, and L. B. Godefroid, “Fatigue crack growth analysis of pre-strained 7475-T7351 aluminum alloy,” *International Journal of Fatigue*, vol. 28, no. 8, pp. 934–942, 2006.

[12] S.-P. Zhu, Q. Lei, H.-Z. Huang, Y.-J. Yang, and W. Peng, “Mean stress effect correction in strain energy-based fatigue life prediction of metals,” *International Journal of Damage Mechanics*, vol. 26, no. 8, pp. 1219–1241, 2017.

[13] S. P. Zhu, Q. Lei, and Q. Y. Wang, “Mean stress and ratcheting corrections in fatigue life prediction of metals,” *Fatigue & Fracture of Engineering Materials & Structures*, vol. 40, no. 9, pp. 1343–1354, 2017.

[14] J. A. F. O. Correia, P. J. Huffman, A. M. P. De Jesus et al., “Unified two-stage fatigue methodology based on a probabilistic damage model applied to structural details,” *Theoretical and Applied Fracture Mechanics*, vol. 92, pp. 252–265, 2017.

[15] N. E. Dowling, C. A. Calhoun, and A. Arcari, “Mean stress effects in stress-life fatigue and the Walker equation,” *Fatigue & Fracture of Engineering Materials & Structures*, vol. 32, no. 3, pp. 163–179, 2009.

[16] N. E. Dowling, “Mean stress effects in strain-life fatigue,” *Fatigue & Fracture of Engineering Materials & Structures*, vol. 32, no. 12, pp. 1004–1019, 2009.

[17] R. Burger and Y.-L. Lee, “Assessment of the mean-stress sensitivity factor method in stress-life fatigue predictions,” *Journal of Testing and Evaluation*, vol. 41, no. 2, 2013.

[18] J. Correia, N. Apetre, A. Arcari et al., “Generalized probabilistic model allowing for various fatigue damage variables,” *International Journal of Fatigue*, vol. 100, pp. 187–194, 2017.

[19] J. A. F. O. Correia, S. Blasón, A. M. P. De Jesus, A. F. Canteli, P. M. G. P. Moreira, and P. J. Tavares, “Fatigue life prediction based on an equivalent initial flaw size approach and a new normalized fatigue crack growth model,” *Engineering Failure Analysis*, vol. 69, pp. 15–28, 2016.

[20] L. Susmel, “Multiaxial fatigue limits and material sensitivity to non-zero mean stresses normal to the critical planes,” *Fatigue & Fracture of Engineering Materials & Structures*, vol. 31, no. 3-4, pp. 295–309, 2008.

[21] A. Niesłony and M. Böhm, “Mean stress effect correction using constant stress ratio S-N curves,” *International Journal of Fatigue*, vol. 52, pp. 49–56, 2013.

[22] D. Kujawski, “A deviatoric version of the SWT parameter,” *International Journal of Fatigue*, vol. 67, pp. 95–102, 2014.

[23] M. Kamaya and M. Kawakubo, “Mean stress effect on fatigue strength of stainless steel,” *International Journal of Fatigue*, vol. 74, pp. 20–29, 2015.

[24] A. Ince, “A mean stress correction model for tensile and compressive mean stress fatigue loadings,” *Fatigue & Fracture of Engineering Materials & Structures*, vol. 40, no. 6, pp. 939–948, 2017.

[25] M. Nihei, P. Heuler, C. Boller, and T. Seeger, “Evaluation of mean stress effect on fatigue life by use of damage parameters,” *International Journal of Fatigue*, vol. 8, no. 3, pp. 119–126, 1986.

[26] K. Kluger and T. Lagoda, “A new algorithm for estimating fatigue life under mean value of stress,” *Fatigue & Fracture of Engineering Materials & Structures*, vol. 40, no. 3, pp. 448–459, 2017.

[27] S.-J. Wang, M. W. Dixon, C. O. Huey, and S.-C. Chen, "The clemson limit stress diagram for ductile parts subjected to positive mean fatigue loading," *Journal of Mechanical Design*, vol. 122, no. 1, pp. 143–146, 2000.

[28] J. A. F. O. Correia, P. Raposo, M. Muniz-Calvente et al., "A generalization of the fatigue Kohout-Věchet model for several fatigue damage parameters," *Engineering Fracture Mechanics*, vol. 185, pp. 284–300, 2017.

[29] R. W. Landgraf, "The resistance of metals to cyclic deformation," in *Achievement of High Fatigue Resistance in Metals and Alloys*, ASTM STP 467. American Society for Testing and Materials, pp. 3–36, Philadelphia, Pa, USA, 1970.

[30] S. K. Koh and R. I. Stephens, "Mean stress effects on low cycle fatigue for a high strength steel," *Fatigue & Fracture of Engineering Materials & Structures*, vol. 14, no. 4, pp. 413–428, 1991.

[31] A. Ince and G. Glinka, "A modification of Morrow and Smith-Watson-Topper mean stress correction models," *Fatigue & Fracture of Engineering Materials & Structures*, vol. 34, no. 11, pp. 854–867, 2011.

[32] O. H Basquin, "The exponential law of endurance tests," *American Society Testing Mater Proceedings*, vol. 10, pp. 625–630, 1910.

[33] Z. Lv, H.-Z. Huang, H.-K. Wang, H. Gao, and F.-J. Zuo, "Determining the Walker exponent and developing a modified Smith-Watson-Topper parameter model," *Journal of Mechanical Science and Technology*, vol. 30, no. 3, pp. 1129–1137, 2016.

[34] *The High Temperature Material Branch of Chinese Society for Metals. China Superalloys Handbook*, China Standard Press, Beijing, China, 2012.

[35] *Editorial Committee for the Material Data Handbook for Areo-Engine Design, Material Data Handbook for Aero-engine Design*, Aviation Industry Press, Beijing, China, 2010.

[36] B. J. Lazan and A. A. Blatherwick, *Fatigue properties of aluminum alloys at various stress ratios," Part 1, rolled alloys. WADC TR 52-307, Part 1*, Wright Air Development Center. Wright-Patterson AFB, Dayton, Ohio, USA, 1952.

[37] L. Susmel, "The theory of critical distances: a review of its applications in fatigue," *Engineering Fracture Mechanics*, vol. 75, no. 7, pp. 1706–1724, 2008.

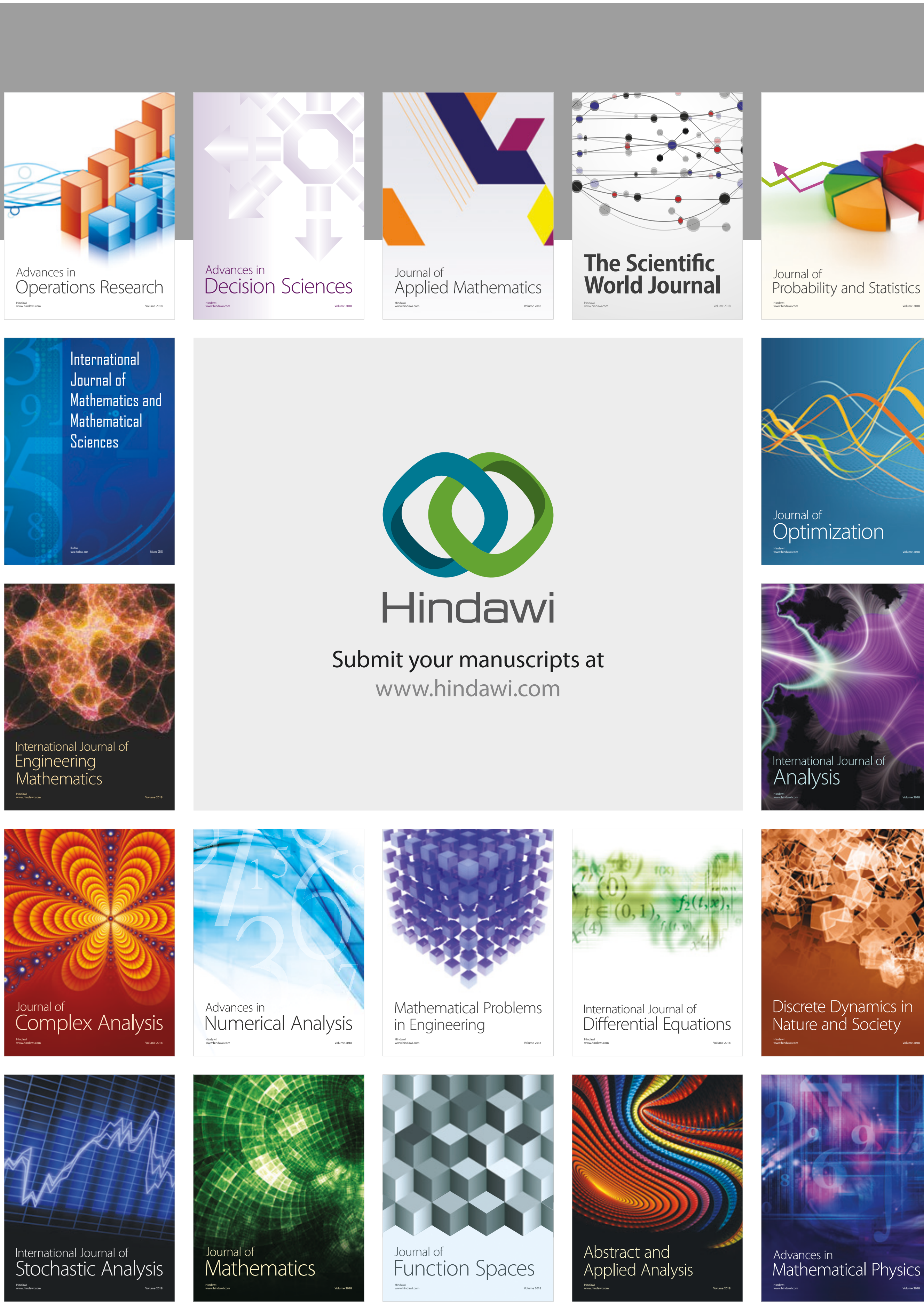
Advances in
Operations Research
Advances in
Decision Sciences
Journal of
Applied Mathematics
The Scientific
World Journal
Journal of
Probability and Statistics
International
Journal of
Mathematics and
Mathematical
Sciences
Hindawi
Submit your manuscripts at
www.hindawi.com
Journal of
Optimization
International Journal of
Engineering
Mathematics
International Journal of
Analysis
Journal of
Complex Analysis
Advances in
Numerical Analysis
Mathematical Problems
in Engineering
International Journal of
Differential Equations
Discrete Dynamics in
Nature and Society
International Journal of
Stochastic Analysis
Journal of
Mathematics
Journal of
Function Spaces
Abstract and
Applied Analysis
Advances in
Mathematical Physics